EVALUATION OF JET MIXING RATE BASED ON DNS DATAS OF EXCITATION JETS

Koichi Tsujimoto
Division of Mechanical Engineering ,
Graduate School of Engineering, Mie University
1577 Kurimamachiya-cho, Tsu, 514-8507 Japan
tujimoto@mach.mie-u.ac.jp

Shuji Kariya, Toshihiko Shakouchi and Toshitake Ando
Division of Mechanical Engineering ,
Graduate School of Engineering, Mie University
1577 Kurimamachiya-cho, Tsu, 514-8507 Japan

ABSTRACT

To establish a good measure of mixing rate, jet mixing is examined based on the DNS (direct numerical simulation) data of the controlled jets. In the computation, the spatial discretization is performed by hybrid scheme in which sixth order compact scheme in streamwise direction and Fourier series in cross section are adopted. The Reynolds number is 1500. The mixing properties are estimated by two measures such as a statistical entropy and a mixedness parameter, which are constructed based on the concentration of the passive scalar. Compared with simple measures,*i.e.*, jet width, centerline velocity and turbulent kinetic energy, it is found that the statistical entropy is a good measure to describe the mixing state in the different controlled jets and that the fluctuating entropy enable to express the highly mixed region and correlates to the vortical structure. As well as the statistical entropy, the mixedness parameter also has useful properties for the estimation of mixing efficiency. These findings suggest that these measures are expected to contribute to the optimization of jet mixing.

INTRODUCTION

In order to enhance mixing or diffusion in many industrial applications, jet mixing control has been examined. The control methodology of the jet mixing is categorized into either passive or active means. Despite the methodology,it is indispensable to grasp the mixing state to realize the effective jet control. From the results of liner stability analysis, it reveals that two types of dominant mode characterizing the large-scale flow structures near field of the jet are varicose and helical mode, and that the diffusion or the mixing is effectively controlled using these modes. Further it is well-known that the assemble of these mode is able to make the complex jet (Reynolds,2003). For example a pair of helical mode having the same frequency and amplitude causes the flapping mode. Further adding the axial mode to them, the occurrence of bifurcating or blooming jet is experimentally confirmed (Reynolds,2003). Such an active control was also investigated using DNS(direct numerical simulation) (Hilgers,2001, Silva,2002), and reported the generation of strong diffusion.

Although the effectiveness of these control is demonstrated so far, simple estimation by the jet width, mean streamwise velocity, turbulence intensity and so on, are conducted only and it is not well enough to evaluate the mixing efficiency based on the reliable procedure. Also we investigate compound jets(Tsujimoto,2006) and experience that the mixing efficiency is not determined with the order of superiority by using the simple measure based on the axisymmetric jet. Thus it is important to investigate the appropriate measure to quantify the mixing efficiency.

When we consider the mixing states, we simply expect that a concentration of passive scalar enable to accurately represent the state of diffusion for the quantification of jet mixing. Then in the present paper, we pick up as new measures, the statistical entropy (Everson,1998) and the mixedness parameter (Tseng,2001) and demonstrate the validity and usefulness of these measures compared to the conventional measures.

NUMERICAL METHOD

Governing equation and discretization

Under the assumption of incompressible and isothermal flow, the dimensionless governing equations are as follows:

$$\frac{\partial u_i}{\partial x_i} = 0 \tag{1}$$

$$\frac{\partial u_i}{\partial t} + h_i = -\frac{1}{\rho}\frac{\partial p}{\partial x_i} + \frac{1}{Re}\frac{\partial^2 u_i}{\partial x_j^2} \tag{2}$$

$$(h_i = \epsilon_{ijk}\omega_j u_k, \quad \omega_j : \text{vorticity})$$

$$\frac{\partial T}{\partial t} + \frac{\partial u_i T}{\partial x_i} = \frac{1}{RePr}\frac{\partial^2 T}{\partial x_i^2} \tag{3}$$

The nonlinear terms are written in the rotational form $\omega \times \mathbf{u}$ to conserve the total energy; thus, p represents the total pressure. As the characteristic length and velocity, the nozzle diameter,D and the streamwise velocity,$V_0 = V_1 - V_2$ (referred to eq.(4)) are chosen for nondimensionalization. The Reynolds number is defined as $Re = V_0 D/\nu$ (ν: dynamic viscosity). A Cartesian coordinate system is employed, in which y is streamwise direction and x, z are in the lateral directions. The spatial discretization is performed by hybrid scheme in which sixth order compact scheme (Lele, 1992) in the streamwise direction and Fourier series in the lateral directions are adopted. In order to remove the numerical instability due to the nonlinear terms, the 2/3-rule is applied for the lateral directions and an implicit filtering for the

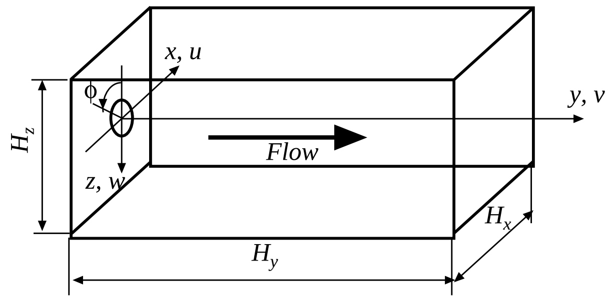

Fig.1 Coordinate system and computational domain.

streamwise direction is conducted with 6th order compact scheme. For the time advancement, third order Adams-Bashforth method is used. The well-known MAC method is employed for pressure-velocity coupling, which results in a Poisson equation for the pressure. After the Poisson equation is Fourier transformed in x, zdirections, the independent differential equations are obtained for each wave number and then is discretized with sixth order compact scheme. Finally the pentadiagonal matrix are deduced for each wave number. In the present simulation code, these matrix are solved using the LU Decomposition method. The outerflow boundary condition is introduced for both momentum and energy equations by solving simplified convective equations.

Calculation conditions

As inflow condition, the inflow velocity distribution is determined by referring the literature (Silva, 2002).

$$V_b(r) = \frac{V_1 + V_2}{2} - \frac{V_0}{2} \tanh\left[\frac{1}{4}\frac{R}{\theta_0}\left(\frac{r}{R} - \frac{R}{r}\right)\right] \tag{4}$$

where V_1 is the jet centerline velocity, V_2 is a co-flow velocity, V_0 means $V_0 = V_1 - V_2$. $R(= D/2)$ is the jet radius and θ_0 is the momentum thickness of the initial shear layer. r denotes the radial distance from the jet centerline. In the present simulations, jet velocity and the initial momentum thickness are set to $V_1 = 1.075V_0$, $V_2 = 0.075V_0$ and $R/\theta_0 = 20$, respectively. The inflow temperature is prescribed by the same distribution of inlet velocity,V_b. The size of computational domain is set to $H_x \times H_y \times H_z$ =$7D \times 15D \times 7D$ except for the flapping excitation case($H_x = H_z = 10D$ for the flapping case). The grid number, $N_x \times N_y \times N_z$ is $256 \times 200 \times 256$. The Reynolds number is $Re = 1500$ and the Prandtl number, $Pr = 0.707$.

Excitation types

In order to enhance the mixing using active control, three types of excitation, $i.e.$ axial (V_a), helical (V_h) and flapping (V_f) excitation are considered. In each excitation, the following perturbation velocity and a random perturbation having 1% strength of the inflow velocity are superposed on the inlet velocity, V_b.

$$\begin{aligned} V_a &= \varepsilon_a \sin(2\pi St_a t^*)V_b && (5) \\ V_h &= \varepsilon_h \sin(\phi - 2\pi St_h t^*)V_b && (6) \\ V_f &= \varepsilon_f \left[\sin(\phi - 2\pi St_f t^*) - \sin(\phi + 2\pi St_f t^*)\right] V_b && (7) \end{aligned}$$

where t^* means a nondimensionalized time, $t^* = tV_0/D$, and $\varepsilon_{a,h,f}$ is the strength of excitation. ϕ is the azimuthal angle shown in Fig. 1. The Strouhal number, $St_{a,h,f}$ is defined as $St = fD/V_0$ (where f: frequency). According to the each excitation, it is well-known that the peculiar instability mode is induced near field of the jet.; In the case of axial excitation, the column of vortex rings is formed upstream, and in the case of helical excitation, the helical-like vortical structures appear. In the case of flapping excitation, flow structures are distorted in one radial direction and the the strong anisotropic mixing occurs downstream.

The frequency of instability mode associated with the generation of large-scale structures induced by the column instability near the end of potential core of jet, is so-called 'preferred mode'. Since the preferred mode is influenced by the shape of nozzle or the boundary layer near the nozzle exit, the preferred mode, St_p becomes $0.25 < St_p < 0.5$ (Hussain et al.,1998). In the present simulation, the excitation frequency are set to $St_a = St_h = St_f = 0.4$, the strength of excitation, $\varepsilon_a = \varepsilon_h = \varepsilon_f = 0.05$.

Mixing measures based on the concentration of passive scalar

Statistical entropy. In order to quantify the mixing state, Everson et al.(1998) pay attention the statistical entropy based on the concentration of the passive scalar, and demonstrate the characteristics of this measure by examining the experimental data. In the followings, we simply explain the content of this measure.

Boltzmann proposed the statistical entropy which is defined as the logarithm of combination, W.

$$S = k \ln W \tag{8}$$

where k is Boltzmann constant. $W$is the combination of the particle number in i^{th} coarse-grained cell, N_i.

$$W = \frac{N!}{N_1!N_2!\cdots N_M!} = \frac{N!}{\prod N_i!} \tag{9}$$

where N is total number of particles. If $N$is enough large, Stirling's approximation,$\ln L! \approx L\ln L - L$ can be applied to eq.(8);

$$S = k\left[N\ln N - \sum_{i=1}^{M} N_i \ln N_i\right] \tag{10}$$

If the space is divide to M's cell and all particles exist only one cell, $S_{min} = 0$. While, if the particles uniformly distribute in each cell, $i.e.$, $N_i = N/M$, the maximum entropy, $S_{max} = kN\ln M$ is attained. Since the incompressible flow is assumed in the present study, the temperature can be related to the concentration of the passive scalar, $\phi = (T - T_2)/(T_1 - T_2)$. Considering the small volume surrounding a grid point,i, $\Delta V(= \Delta x\Delta y\Delta z)$, the particle number denotes $N_i = \phi_i \Delta V$, thus

$$S = k\Delta V\left[\Phi\ln\Phi - \sum_{i=1}^{M}\phi_i \ln\phi_i\right] \tag{11}$$

where $\Phi = \sum \phi_i$.

Mixedness parameter. Tseng et al.(1998) defined the mixedness parameter,Mp;

$$Mp = \frac{1}{V}\int_V \phi(1-\phi)dV \tag{12}$$

where V is the total volume of the considering domain. For completely unmixed state, $Mp_{min} = 0$ and for fully mixed

(a) Normal

(b) Axial excitation

(c) Helical excitation

(d) Flapping excitation

Fig.2 Instantaneous vortex structure visualized at Q=0.2.

state $Mp_{max} = 0.25$. Compared to the statistical entropy, it is seem that Mp is intuitively derived.

RESULTS

Structure of controlled jets

In order to visualized the vortical structure, iso-surfaces of velocity gradient tensor, Q value are shown in Fig. 2. In each figures, left means the side view, right the view from the nozzle side. In Fig. 2(a), due to a Kelvin-Helmholtz instability occurred upstream, quasi-periodically vortex-ring like structures are generated. As the vortex rings break down downstream, then tube like vortical structures are formed. In case of axial excitation (Fig.2(b)), depending on the excitation frequency, the strong vortical structures regularly are formed and retained for a while from upstream to downstream. From this figure, vortex rings do not successively interact with each other. However as well as non-excitation, when the vortex ring rapidly break down, the formation of quasi-streamwise vortices is observed downstream. In case of helical excitation (Fig. 2(c)), the helical like structures continuously are formed from the upstream to the downstream. The break down of this case occurs earlier than the above-mentioned cases, because the streamwise vorticity component is included at earlier stage of the evolution. In case of flapping excitation (Fig.2(d)), the jet markedly

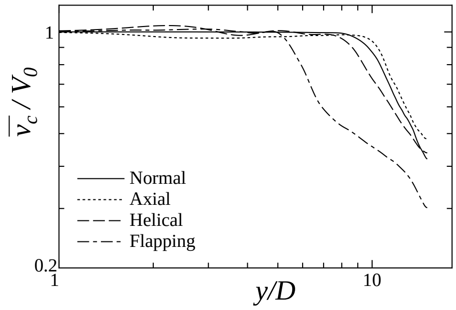

Fig.3 Distribution of mean centerline velocity.

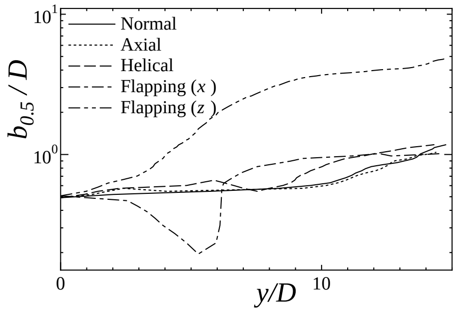

Fig.4 Distribution of half jet width.

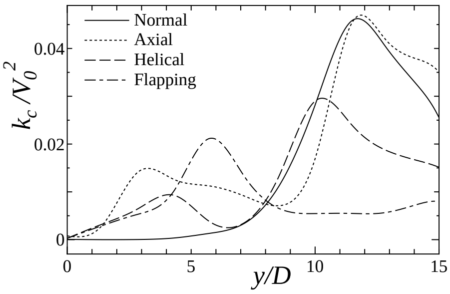

(a)

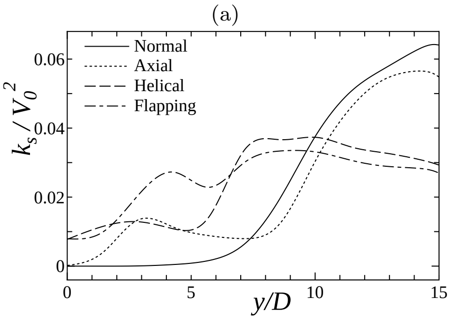

(b)

Fig.5 Distribution of turbulence kinetic energy, (a) centerline value and (b) integrated value with eq(13).

diffuses for one direction. The reason is that after the issuing from the nozzle, strong hair-pin like structures are alternately formed upstream.

The visualized flow structures of all cases are in accordance with the previous DNSs(Silva,2002, Urban,1997), therefore the present results are confirmed to be correct under the giving excitation conditions.

Simple measure for jet mixing

As the measure of mixing rate, flow properties such as centerline velocity, jet width and turbulence intensity have been considered. Fig. 3 shows the distribution of centerline

velocity, $\bar{v}_c = \bar{v}(0, y, 0)$. Corresponding to the visualized coherent structures, the breakdown position of potential core in the flapping case, $y/D \approx 5$ locates more upstream than the other case. Except for the flapping case, the break down position is shifted downstream in order of the helical, the normal and the axial excitation. In particular, contrary to our intuition, the decay of centerline velocity in axial excitation case is shifted downstream compared to the normal case. As might be expected, the starting position of decay of velocity are largely delay compared to the visualized structure.
The jet half width, $b_{0.5}$ is shown in Fig.4. In both the normal and the axial excitation case, the jet expands at same rate from a downstream position ($y/D = 10$) at which the ring-like vortex structures begin to break down. While in the helical excitation case, although the half-width behaves singularly near $y/d = 5$ at which vortex break down occurs, roughly saying, the jet widely expand than both normal and axial case. In the flapping case, the jet markedly expands for one direction (z), and shrinks for the perpendicular to the another direction(x), demonstrating anisotropic distribution. Not shown here, the shrinks of jet width in x direction is confirmed from iso-contour of mean streamwise velocity. Compared to the centerline velocity distribution, the jet width enables to capture the diffusion rate, however, if the anisotropic pattern of jet diffusion occurs, or if jets is combined, it is difficult to uniquely define the jet width, suggesting that the estimation using the jet width is limited for a simplified jet.

Figures 5 show the distribution of turbulent kinetic energy (TKE), $k(= \frac{1}{2}u'^2_{i,rms})$. Fig. 5(a) shows centerline distribution of TKE, $k_c = k(0, y, 0)$. In all excitation case, the turbulence is strongly generated by the coherent structure induced by the excitation near $y/D \approx 5$. Corresponds to the visualized structures, in the case of normal, axial and helical excitations, turbulence generation is rapidly promoted downstream as the breakdown of vortical structures proceed. While in the flapping case, since the vortex break down considerably proceeds than the other case, the secondary peak downstream does not appear. Fig. 5(b) show the distribution of integrated turbulent kinetic energy defined with eq.(13).

$$k_s = \int_{-H_z/2}^{H_z/2} \int_{-H_x/2}^{H_x/2} \frac{1}{2} k dx dz \qquad (13)$$

Considering the mixing state, the flapping case should be most enhanced, however, the amount of turbulent kinetic energy in both helical and flapping cases are obviously less than the normal and axial case. In general the generation of turbulent kinetic energy is determined by the product of mean shear and the Reynolds stresses. Since the mean shear is more weaken if the break down is more promoted, thus the amount of turbulence does not always increase.

These findings suggests that turbulence intensity gives the information of the position where the the mixing is enhanced, but not became the qualitative measure for the mixing rate.

Evaluation the mixing measure based on the passive scalar

We evaluate the above mentioned measure,*i.e.*, the statistical entropy and the mixedness parameter. In order to investigate the streamwise variation of the statistical entropy, S is summed over the plane perpendicular to the streamwise direction, and $\overline{S}$ is defined as S normalized with

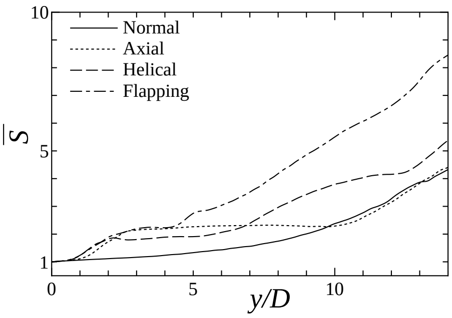

(a)

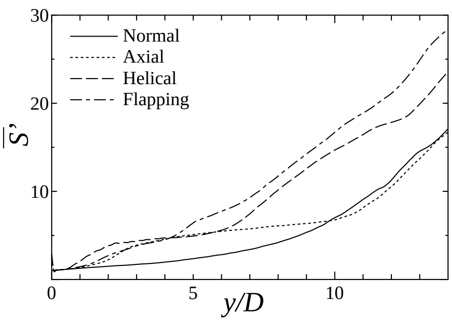

(b)

Fig.6 Distribution of (a) total entropy and (b) fluctuating entropy.

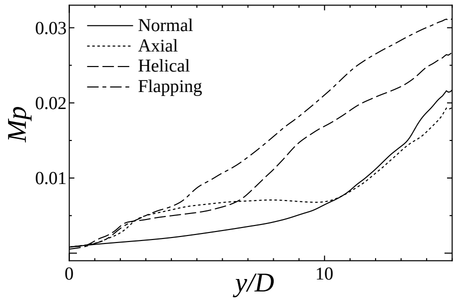

Fig.7 Distribution of mixedness parameter.

the inflow quantity, S_0. M means a grid number on $x - z$ plane; M=65, 536(= 256×256). From Fig.6(a) the statistical entropy increase downstream in order of the axial, the helical and the flapping case. These futures reflect in the increase of randomness downstream and the mixing enhancement due to the excitations. In particular, in the axial excitation, the entropy increases until $y/D = 2$, and then became nearly constant until $y/D = 10$. The reason is that the vortical structures move downstream without the break down, and it suggests that the aggressive formation of vortex ring does not always contribute to the promotion of jet mixing.

Here it should be noted that the first term of *r.h.s* in eq.(10) express the total number of particles, N and two orders of magnitude larger than second term of *r.h.s.*. When the larger the total number of particles exists, the statistical entropy increases. Namely, this measure reflects the physical property corresponding to the jet expansion. However if the same number of particles are distributed between different jets, the first terms of eq.(10) does not represent the difference concerning the mixing property, thus it seem that the second term of eq.(10) includes the substantial properties for

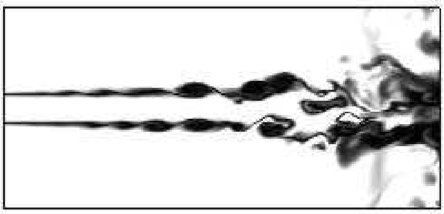

(a) Normal

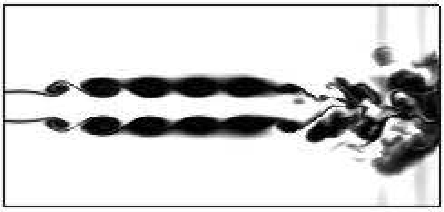

(b) Axial excitation

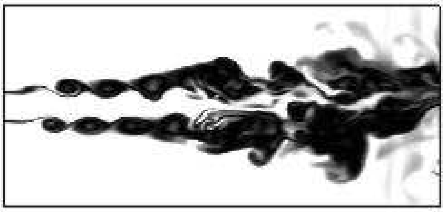

(c) Helical excitation

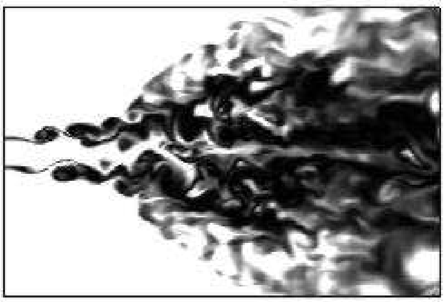

(d) Flapping excitation

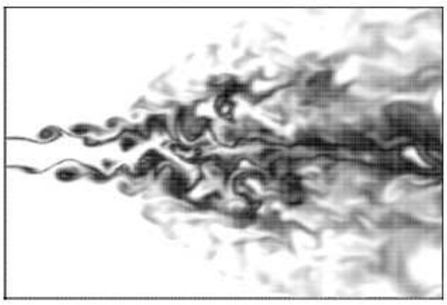

(e) Flapping excitation

Fig.8 Contour of ingredient of mixing measure on x-y plane, (a)-(d) for the statistical entropy, (e) for the mixedness parameter.

mixing, despite that the order of this term is smaller than the first one.

The second term is defined as fluctuating entropy, S':

$$S' = -\sum_{i=1}^{M} \phi_i \ln \phi_i \tag{14}$$

As similar to the Fig.6(a), $\bar{S}'$ is defined as the quantity S' normalized with the inlet value. From Fig. 6, $\bar{S}'$ and $\bar{S}$ are not quantitatively but qualitatively similar.

Fig. 7 shows the distribution of mixedness parameter which is defined by integrating the component,$\phi(1-\phi)$ on cross sectional $(x-z)$plane. Although there is a quantitative difference between two measures, it is found that the trend of the mixedness parameter behaves similar to that of the statistical entropy. Despite that the derivation of two measures are distinct, both parameters enable to prioritize the efficiency for the jet mixing.

Relation between the mixing measure and the flow structure

Figures 8(a)-(d) show the iso-contour of the component of fluctuating entropy, $-\phi \ln \phi$, on the $y-z$ plane through the jet centerline. Also Fig.8(e) is for that of the mixedness parameter. In all cases, it is found that the component of fluctuating entropy becomes strong in the region where the strong shear near the inlet exists and where the vortical structures are generated, and that further downstream mixing measure distribute according to the jet expansion. Also it is clarified that except for flapping case, the mixing makes no progress near the jet axis.

Although from Fig. 5, the turbulence near the jet axis become strong at earlier stage of flow development, it does not effectively contribute to the jet mixing, and the mixing is enhanced in the region only where the entrainment of surroundings are active. Further downstream, because of the entrainment, the mixing is enhanced even in the near the jet axis and the flow becomes more chaotic. From Fig.8(e), we also confirm that the mixedness parameter has a similar trend as the statistical entropy.

Since these measure are convected to the downstream, the mixing is affected by the history of upstream and their upstream effect is accumulated for downstream. Thus we consider the production rate of mixing measure based on the transport equations of mixing measure. Converting the temperature to the scalar concentration, the transport equations of mixing measure are derived as follows:

$$\frac{D(-\phi \ln \phi)}{Dt} = \frac{1}{RePr}\left[\nabla^2(-\phi \ln \phi) + \frac{(\nabla\phi)^2}{\phi}\right] \tag{15}$$

Similar for the mixedness parameter:

$$\frac{D\phi(1-\phi)}{Dt} = \frac{1}{RePr}\left[\nabla^2\{\phi(1-\phi)\} + 2(\nabla\phi)^2\right] \tag{16}$$

In both equations, the first term of $r.h.s$ expresses the diffusion and do not contribute to the substantial change of mixing measure. Since the second terms are always positive value, they represent the substantial production term of mixing measure. Note that the second terms express the scalar dissipation, and that the generation of the mixing is related to the region where the gradient of scalar becomes strong.

Figures 9(a)-(d) show the iso-contour of the second terms of $r.\ h.\ s.$ in eq.(15), $\frac{1}{RePr\phi}(\nabla\phi)^2$. Figure 9(e) shows that of the mixedness parameter. Upstream high value of this term distributes in relation to the high shear around vortical structures, in particular, the higher value one seems to be relate to the region where the stretching between vortical structures are enhanced. Further downstream the distribution seems to be chaotic as similar to Fig.8. The enhanced production region is located locally near the beginning of vortex break down. Also that of mixedness parameter behave similar to that of the statistical entropy. In order to activate the mixing, since the gradient of scalar should become

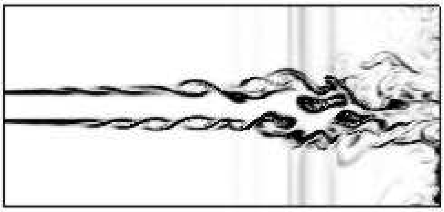

(a) Normal

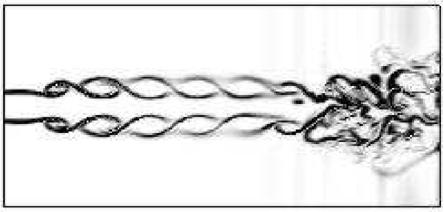

(b) Axial excitation

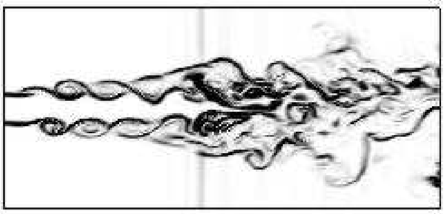

(c) Helical excitation

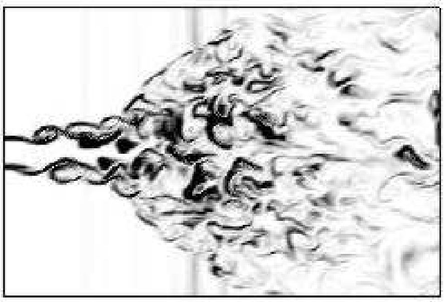

(d) Flapping excitation

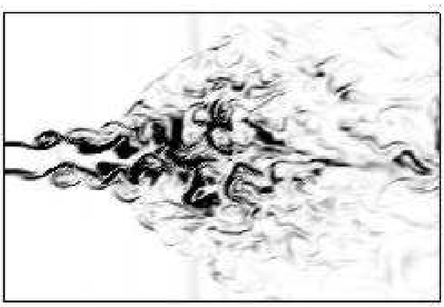

(e) Flapping excitation

Fig.9 Contour of production term of mixing measure on x-y plane, (a)-(d) for the statistical entropy, (e) for the mixedness parameter.

strong to enhance the molecular diffusion, the stretching should be enhanced. Since these measures are in accordance with the well-known physical properties of jet mixing, and at the same time it is expected that the local mixing state is comprehended to establish the control methodology.

CONCLUSIONS

We investigate the measure of jet mixing based on the concentration of passive scalar using the DNS databases of controlled jets. Conclusions are as follows:

1. The simple measure for mixing state, such as the centerline velocity, the jet width and the turbulence intensity are a rough index. However, since their measure are constructed based on the axisymmetric jet, they are not useful to compare the mixing efficiency for the complex jet such as flapping case.

2. As the mixing measure based on the passive scalar, the statistical entropy and the mixedness parameter are investigated. As a consequence it is demonstrated that these measures have the similar ability to correctly evaluate the mixing efficiency between different jets.

3. From the instantaneous view of the component of these mixing measure, these quantities and the production terms of their transport equation also strongly correlate the vortical structures, suggesting that the components of these new measures enable to detect the local mixed state.

REFERENCES

Everson, R., Manin, D. and Sirovich, L., 1998, "Quantification of Mixing and Mixing Rate from Experimental Observations", *AIAA J.* Vol. 36, pp. 121-127.

Hilgers, A. and Boersma, B. J., 2001, "Optimization of turbulent jet mixing", *Fluid Dyn. Res.*, Vol. 29, pp. 345-368.

Hussain, A. K. M. F. & Zaman, K. B. M. Q., *Phys. Fluid* **10** (1998), pp.899-909.

Lele, S. K., 1992, "Compact finite difference schemes with spectral-like resolution", *J. of Comp. Phys.* Vol. 103, pp. 16-42.

Reynolds, W. C., Parekh, D. E., Juvet, P. J. D. and Lee, M. J. D., 2003, "Bifurcating and Blooming Jets", *Annu. Rev. Fluid Mech.*, pp. 295-315.

Roshko, A., 1976, "Structure of Turbulent Shear Flows : A New Look", *AIAA J.* Vol. 14, pp. 1349-1357.

Silva, C. B. and Metais, O., 2002, "Vortex control of bifurcating jets: A numerical study", *Phys. of Fluids*, Vol. 14, pp. 3798-3819.

Tseng, Y. and Ferziger, J., H., 2001, "Effects of Coastal Geometry and the Formation of Cyclonic/Anti-Cyclonic Eddies on Turbulent Mixing in Upwelling Simulation", *J. Turbulence* Vol. 2-014, pp. 1-23.

Tsujimoto, K., Shakouchi, T. Sasazaki S and Ando, T., 2006, "Direct Numerical Simulation of Jet Mixing Control Using Combined Jets", *JSME Int. J. Ser. B*, Vol. 49-4, pp. 966-973.

Urbin, G. and Metais O., 1997, "Large-eddy simulations of three-dimensional spatially-developing round jets", *In Direct and large-eddy simulations* **II**, P.R. Chollet, J.P.Voke and L. Kleiser, Kluwer: Dordrecht, pp. 539-542.